PCCP

ROYAL SOCIETY OF CHEMISTRY

PAPER

View Article Online
View Journal | View Issue

Published on 05 October 2020. Downloaded by University of Colorado at Boulder on 5/26/2021 9:49:42 PM.

Check for updates

Cite this: *Phys. Chem. Chem. Phys.*, 2020, **22**, 23491

Single-molecule kinetic studies of DNA hybridization under extreme pressures†

Hsuan-Lei Sung[ab] and David J. Nesbitt *[abc]

Received 29th July 2020,
Accepted 5th October 2020

DOI: 10.1039/d0cp04035e

rsc.li/pccp

Hydrostatic pressure can perturb biomolecular function by altering equilibrium structures and folding dynamics. Its influences are particularly important to deep sea organisms, as maximum pressures reach ≈1100 bar at the bottom of the ocean as a result of the rapid increase in hydraulic pressure (1 bar every 10 meters) under water. In this work, DNA hybridization kinetics has been studied at the single molecule level with external, tunable pressure control (P_{max} ≈ 1500 bar), realized by incorporating a mechanical hydraulic capillary sample cell into a confocal fluorescence microscope. We find that the DNA hairpin construct promotes unfolding ("denatures") with increasing pressure by simultaneously decelerating and accelerating the unimolecular rate constants for folding and unfolding, respectively. The single molecule kinetics is then investigated *via* pressure dependent van't Hoff analysis to infer changes in the thermodynamic molar volume, which unambiguously reveals that the effective DNA plus solvent volume increases ($\Delta V^0 > 0$) along the folding coordinate. Cation effects on the pressure dependent kinetics are also explored as a function of monovalent [Na^+]. In addition to stabilizing the overall DNA secondary structure, sodium ions at low concentrations are also found to weaken any pressure dependence for the folding kinetics, but with these effects quickly saturating at physiologically relevant levels of [Na^+]. In particular, the magnitudes of the activation volumes for the DNA dehybridization ($\Delta V^{\ddagger}_{unfold}$) are significantly reduced with increasing [Na^+], suggesting that sodium cations help DNA adopt a more fold-like transition state configuration.

I. Introduction

Most biochemical studies are performed under ambient pressures (≈1 bar = 100 000 Pascal), though this is far from conventional conditions in the deepest parts of the ocean (≈1100 bar).[1,2] Indeed, although experimental results obtained at atmospheric pressure are of obvious relevance to life on the surface of the earth, one could argue that most biochemistry studies sample only a quite limited wedge of naturally occurring pressures in biology. Extreme pressure effects on biological systems turn out to be of immense importance to marine life due to the rapid increase of hydraulic pressure (1 bar per 10 meters) under water.[3] As one particularly relevant biophysical impact, molecules such as proteins and nucleic acids may lose the thermodynamic stability of their native folded state under increasing pressure,[4–7] with such pressure-induced changes in conformation known as pressure denaturation.[8,9] Marine organisms, especially deep-sea species, therefore must evolve and adopt protective mechanisms to stabilize biomolecular structures and maintain biochemical function in order to counteract pressure changes due to change in depth profile.[3,10]

DNA occurs in biology primarily in the form of a double helix configuration. Previous studies have shown the response of DNA secondary structure to pressure to vary, depending on the sequence and buffer conditions.[6] While majority of the relatively long/stable DNA double helices exhibit an increasing melting temperature (T_{melt}) with increasing pressure,[11,12] DNA folding with shorter complementary regions is consistently shown to be destabilized (*i.e.*, denatured) by elevated pressure.[13–15] Since structure determines biomolecular function, such pressure denaturation phenomena of shorter nucleic acid sequences could have a potentially enormous impact on cellular function in deep sea marine species. Moreover, structure in hybridized nucleic acid oligos is in fact dynamic rather than static.[16,17] As a result, the destabilization effects of pressure on nucleic acids may not be fully captured by previous observations under equilibrium conditions. Indeed, predictive understanding of such pressure induced changes in conformational structure clearly will require new tools for exploring not just the equilibria but also the kinetics of nucleic acid hybridization/dehybridization, in particular under the impact of high hydraulic pressures relevant to deep sea life. In order to make such kinetic studies of nucleic acid conformational

[a] *JILA, National Institute of Standards and Technology and University of Colorado, Boulder, CO 80309, USA. E-mail: djn@jila.colorado.edu*
[b] *Department of Chemistry, University of Colorado, Boulder, CO 80309, USA*
[c] *Department of Physics, University of Colorado, Boulder, CO 80309, USA*

† Electronic supplementary information (ESI) available. See DOI: 10.1039/d0cp04035e

Published on 05 October 2020. Downloaded by University of Colorado at Boulder on 5/26/2021 9:49:42 PM.

dynamics possible at the single molecule level, we have coupled together two powerful techniques, (i) confocal single molecule Förster resonance energy transfer (smFRET) with (ii) a high-pressure generating system in a small quartz capillary cell. The goal of the present study is to report first results on folding/unfolding kinetics of small nucleic acid constructs at the single molecule level, with pressure as an external control variable up to ≈5 kilobar.[7,15]

The present work builds on previous experimental studies of pressure dependent nucleic acid RNA and DNA folding under equilibrium conditions, made accessible *via* freely diffusing smFRET methods at the single molecule level.[7,13–15] Specifically, these previous studies investigated doubly dye-labeled nucleic acid constructs diffusing in solution, with FRET energy transfer efficiencies (E_{FRET}) sampled one molecule at a time and single molecule E_{FRET} distributions statistically revealing the equilibrium ratio between folded and unfolded states (K_{eq} = [folded]/[unfolded]), as well as its dependence on external pressure and temperature.[7,13–15] In the present work, DNA constructs are tethered onto the inner surface of a square quartz high pressure capillary cell (Fig. 1) instead of freely diffusing in solution. By virtue of this tethering, we can locate the nucleic acid constructs by piezo scanning a focused laser beam in a confocal microscope and thereby interrogate single molecule fluorescence signals over an extended time window.[18,19] Since the photon stream changes color as a function of nucleic acid conformation, the resulting time dependent E_{FRET} "trajectories" contain valuable statistical information on the folded and unfolded dwell time distributions[19,20] which therefore allow us to explore nucleic acid conformational kinetics as a function of pressure.

The organization of this paper is as follows. Section II provides a brief description of the combined high pressure experimental apparatus and single molecule microscope. This is followed by a presentation in Sections IIIA and IIIB of folding and unfolding kinetic results and analysis as a function of external hydraulic pressure, for which the pressure dependent folding/unfolding kinetics provides detailed quantitative information on the differential molar volumes ($\Delta V^{\ddagger}_{fold}$, $\Delta V^{\ddagger}_{unfold}$) for accessing the transition state from a pressure dependent van't Hoff analysis. We turn in Section IIIC to the impact of "ion atmosphere" on the overall (ΔV^{0}) and transition state ($\Delta V^{\ddagger}$) molar volume changes, which exhibit a strong sensitivity to monovalent Na^{+} but only a surprisingly weak dependence on divalent Mg^{2+}, despite it being crucial for achievement of the correct nucleic acid secondary structure. In Section IV, we discuss the reasons and simple models for such pressure and cationic dependent behaviors, followed in Section V by a summary of the conclusions and directions for further work.

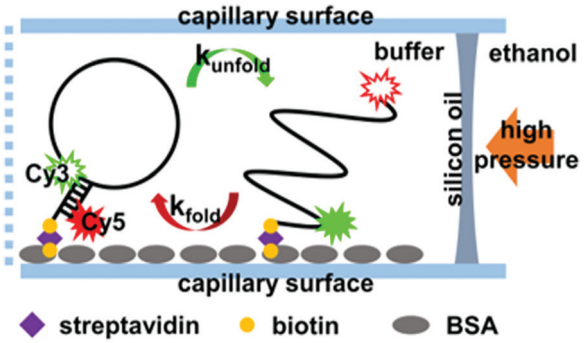

Fig. 1 Schematic presentation of the surface tethered smFRET experiment performed in a pressurized capillary sample holder. The doubly dye-labeled DNA hairpin construct is immobilized on the capillary surface through biotin–streptavidin interactions. The energy transfer efficiency (E_{FRET}) in the folded (left) and unfolded (right) conformations correspond to high E_{FRET} (≈0.8) and low E_{FRET} (≈0.1) fluorescence states, respectively. Prior to each experiment, a thin layer of silicon oil is introduced inside the capillary cell to prevent contamination of the aqueous sample region by the pressure transmitting fluid (ethanol).

II. Experiment

IIA. Single molecule FRET microscopy under external hydraulic pressure

Details of our high pressure smFRET experimental apparatus can be found in previous work;[7,15] we focus herein on modifications required for the present studies of single molecule nucleic acid folding kinetics. In brief, a confocal microscope with a high NA objective is coupled to a high-pressure sample cell fabricated from a fused-silica capillary with a square 50 μm × 50 μm cross section of the inner cell (Polymicro, Phoenix, AZ), where the capillary can sustain pressures up to ≈5 kilobar without fracturing. (Note: company names are mentioned in the interest of completeness and not intended as commercial product support) Moreover, the flat interior surface and uniform thickness (≈155 μm) of the high pressure capillary cell closely approximates that of a standard microscope coverslip configuration, therefore maximizing the excitation/collection efficiency for a high NA (1.2) fluorescence measurement. The aqueous sample is pressurized by a manual screw pump (High Pressure Equipment, Erie, PA) through stainless steel tubing (High Pressure Equipment), with ethanol as pressure transmitting fluid to increase pressurization efficiency. Before connection to the ethanol-filled pressure generating system, one end of the capillary is sealed by a propane/oxygen torch, while the other open end is dipped into low viscosity silicon oil to create a thin liquid membrane (≈50 μm thickness) inside the sample cell (Fig. 1) to prevent diffusion of ethanol into the microscopy region. During the smFRET experiment, the dye-labeled construct is excited by laser excitation through a high NA = 1.2 water immersion microscope objective, with the resulting fluorescence photons collected through the same objective and sorted with dichroic filters before detection on single-photon counting avalanche photodiodes. The time resolved E_{FRET} trajectory is then calculated from the resulting fluorescent signals (Fig. 2) and used in the kinetics analysis described in Section IIIA.

IIB. Sample preparation and single molecule tethering

The doubly dye-labeled and biotinylated DNA hairpin construct has been purchased in HPLC purified form (Integrated DNA Technologies, Coralville, IA) and is used as is.[15,20] More

 This journal is © the Owner Societies 2020

Published on 05 October 2020. Downloaded by University of Colorado at Boulder on 5/26/2021 9:49:42 PM.

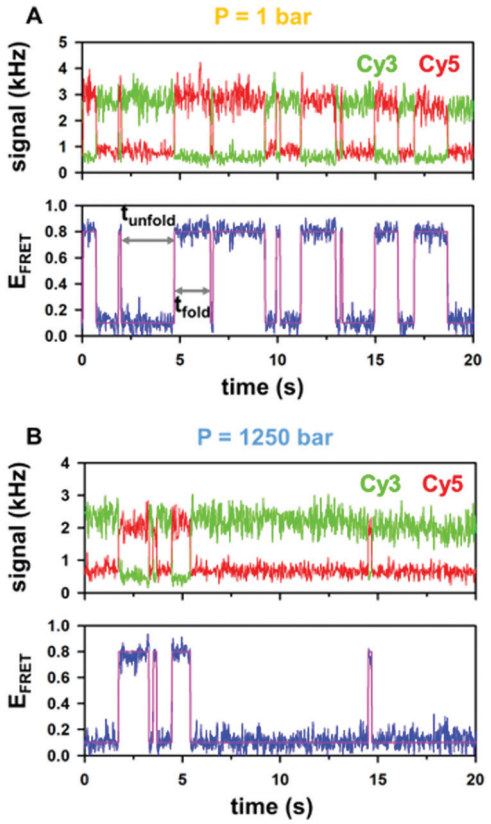

Fig. 2 Sample time-resolved fluorescent signals (upper panels) and corresponding E_{FRET} trajectories (lower panels) at (A) 1 bar and (B) 1250 bar. Background [Na^+] = 50 mmol L^{-1}.

specifically, the construct contains an 8 base pair complimentary sequence separated by a 40-(dA) linker (Fig. 1). The full DNA sequence and dye labeling sites are as follows: 5′-Cy5-TCTTCAGT-A_{40}-Cy3-ACTGAAGA-A10-biotin-3′. The labeling of Cy3 and Cy5 results in two distinct E_{FRET} states corresponding to the folded/hybridized ($E_{FRET} \approx 0.8$) and unfolded/dehybridized ($E_{FRET} \approx 0.1$) conformations.[15,20] To extend the observation time of fluorescent signals from a single construct, the DNA hairpins are immobilized on the surface of the capillary cell through biotin–streptavidin interactions (Fig. 1).[18,19] The DNA hairpin in these first high pressure single molecule kinetic measurements has been widely studied as a model system of nucleic acid secondary structure formation, with the folding kinetics as well as equilibrium behavior extensively characterized under ambient conditions at the single molecule level.[15,20–22] While the incorporation of the poly(dA) linker simplifies the act of DNA hybridization from a bimolecular to unimolecular kinetic process, it may also weakly contribute to the folding kinetics and thermodynamics in addition to duplex formation. Although the ambient folding thermodynamics of the full hairpin construct has been previously shown to be dominated by base paring[15] in the stem, it is worth noting that effects of the linker on the kinetics remain uncharacterized at high pressure.

Preparation of the DNA-decorated surface is achieved by sequentially flushing the capillary cell with the following solutions in order: (i) 10 mg mL^{-1} bovine serum albumin (BSA) with 10% biotinylation for surface passivation, (ii) 200 μg mL^{-1} streptavidin solution for surface immobilization, and (iii) ≈ 25 pmol L^{-1} biotinylated DNA hairpin constructs. Prior to each smFRET experiment, the sample holder is flushed by the imaging buffer containing (i) 50 mmol L^{-1} hemipotassium HEPES buffer (pH 7.5), (ii) trolox/protocatechuate 3,4-dioxygenase (PCD)/protocatechuate (PCA) oxygen scavenger cocktail to catalytically remove oxygen and thereby increase dye photostability, and (iii) sufficient NaCl and $MgCl_2$ to achieve desired monovalent (Na^+)/divalent (Mg^{2+}) cation concentrations. We note that 25 mmol L^{-1} of background K^+ from the HEPES buffer is also present in each of these pressure dependent kinetic experiments.

III. Results and analysis

IIIA. Kinetic origin of DNA hairpin unfolding with increasing pressure

The prolonged observation of a single DNA construct one at a time allows us to obtain the time dependent fluorescence signals from Cy3/Cy5 and calculate the resulting E_{FRET} trajectory (Fig. 2). At ambient (≈1 bar) pressures (Fig. 2A), the correlation between Cy3 and Cy5 fluorescence indicates the DNA hairpin actively switches between the unfolded and folded conformations, corresponding to $E_{FRET} \approx 0.1$ and 0.8, respectively.[15,20] As the pressure increases to 1250 bar (Fig. 2B), the DNA hairpin clearly spends more time in the low E_{FRET} conformation, indicating that the DNA hybridization equilibrium is shifted toward the denatured (*i.e.* unfolded) state with increasing pressure. This is completely consistent with results reported in freely diffusing smFRET studies of similar constructs under equilibrium conditions.[13,15]

However, the present tethered studies contain additional rich information on the folding/unfolding kinetics, which can be extracted by the dwell time analysis with in-house software and thresholding methods (as previously described).[18,19,23] Specifically, the well separated E_{FRET} distributions for the DNA hairpin allow us to unambiguously distinguish between folded/unfolded conformational states with a temporal resolution of 25 ms (Fig. 2A and B). The resulting cumulative distribution functions (CDFs) of dwell time for each of the states are well-fit to a single exponential decay model, as clearly demonstrated by the semi-logarithmic plots in Fig. 3. Thus, both the folding and unfolding of the DNA hairpin appear to follow simple first order kinetics,[20] with the DNA hairpin folding dynamics described by first order rate constants k_{fold} and k_{unfold}, respectively. In Fig. 3A, the CDF slope for the unfolded (red) dwell times is greater than for the folded (green) dwell times ($k_{fold} > k_{unfold}$), and therefore the DNA hairpin spends more time in the folded conformation at ambient pressure with folding equilibrium constant $K_{eq} = k_{fold}/k_{unfold} > 1$. At high pressure (1250 bar, Fig. 3B), the CDF logarithmic decays reveal a dramatic decrease in k_{fold} accompanied by a simultaneous increase in k_{unfold}. Thus, the kinetic origins of pressure induced denaturation of the DNA hairpin are therefore

Published on 05 October 2020. Downloaded by University of Colorado at Boulder on 5/26/2021 9:49:42 PM.

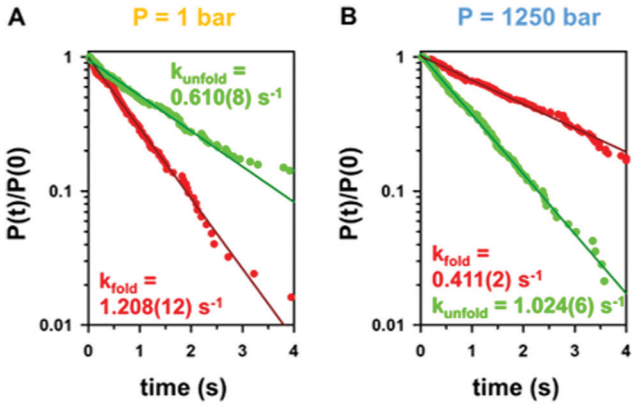

Fig. 3 Sample cumulative distribution functions of dwell time at (A) 1 bar and (B) 1250 bar. Background [Na^+] = 50 mmol L^{-1}.

unambiguously the result of deceleration and acceleration of the folding and unfolding rate constants, respectively.

IIIB. Volumetric characterization of pressure-dependent DNA (un)folding

If we associate the purely single exponential kinetic behavior (Fig. 3) with a single rate-limiting transition state, the rate constant k can be expressed by the Eyring equation[24]

$$k = \nu e^{-\frac{\Delta G^{\ddagger}}{RT}}, \quad (1)$$

where ν represents an approximate attempt frequency to reach the transition state barrier. Since any pressure dependence of the folding/unfolding rate constants and equilibrium constants originates from changes in molar volume along the folding path,[4,5] a more quantitative evaluation can be obtained by van't Hoff analysis of these rate constants at a series of increasing pressures (Fig. 4A):[4,5]

$$\left(\frac{\partial \ln k}{\partial P}\right)_T = \frac{-\Delta V^{\ddagger}}{RT}, \quad (2)$$

where $\Delta V^{\ddagger}_{fold}$ ($\Delta V^{\ddagger}_{unfold}$) represents the activation volume equivalent to volume change from the unfolded (folded) conformation up to the transition state: $\Delta V^{\ddagger}_{fold} = V_{TS} - V_{unfold}$ ($\Delta V^{\ddagger}_{unfold} = V_{TS} - V_{fold}$). As shown in Fig. 4, $\ln(k_{fold})$ decreases linearly as a function of increasing pressure, with the negative slope indicating an increase in volume for the DNA hairpin to reach the transition state barrier from the unfolded state ($\Delta V^{\ddagger}_{fold}$ = +22.1(16) mL mol^{-1}). Conversely, $\ln(k_{unfold})$ increases linearly as a function of pressure, with a slope corresponding to a negative $\Delta V^{\ddagger}_{unfold}$ = −10.3(6) mL mol^{-1}, indicating that the fully folded conformation expands further in molar volume from the transition conformation. Simply summarized, the volumetric analysis of the pressure dependent rate constants reveals that the molar volume of the DNA hairpin increases monotonically along the hybridization path: $V_{unfold} < V_{TS} < V_{fold}$.

Moreover, the conventional pressure-dependent folding equilibrium behavior can be reconstructed simply through the relation $K_{eq} = k_{fold}/k_{unfold}$ (Fig. 4B). The results are consistent

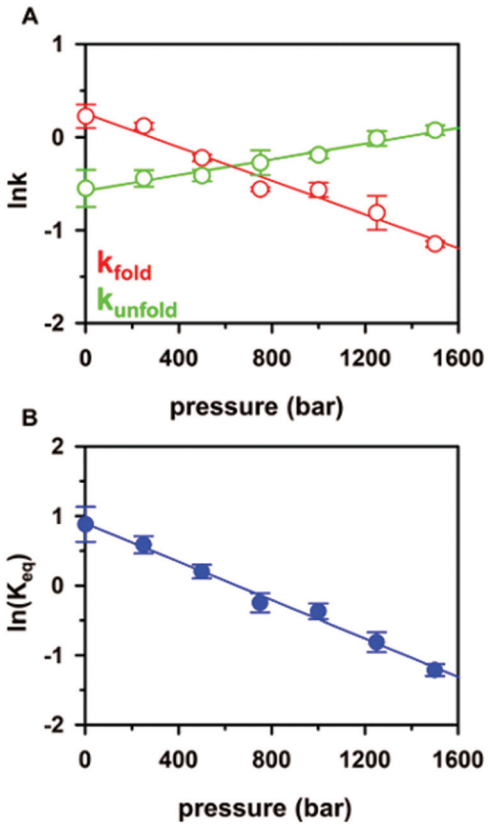

Fig. 4 Pressure dependent van't Hoff analysis of DNA hairpin folding. (A) Folding (k_{fold}) and unfolding (k_{unfold}) rate constants, and (B) folding equilibrium constant (K_{eq}) as a function of increasing pressure. Note that k_{fold} and k_{unfold} are each scaled to 1 Hz (s^{-1}) to permit taking logarithms of unitless quantities. The slope of these plots can be used to infer changes in the molar volume with uncertainties (≈1 to 2 mL mol^{-1}) at ≈5 to 10% of a single H_2O molecule volume (V ≈ 18 mL mol^{-1}). Background [Na^+] = 50 mmol L^{-1}.

with previous observations of $\ln(K_{eq})$ linearly decreasing as a function of increasing pressure[13,15] predicted by[4,5]

$$\left(\frac{\partial \ln K_{eq}}{\partial P}\right)_T = \frac{-\Delta V^0}{RT} \quad (3)$$

The corresponding overall molar volume change upon DNA hairpin folding is found to be ΔV^0 = +33.7(13) mL mol^{-1}, which is in excellent agreement with the present pressure dependent kinetic analysis predictions of $\Delta V^0 = \Delta V^{\ddagger}_{fold} + (-\Delta V^{\ddagger}_{unfold})$ = +32.4(17) mL mol^{-1}. It is worth noting that this overall change in molar volume is substantially higher than found from previous high pressure burst fluorescence studies under equilibrium conditions (ΔV^0 = +23(2) mL mol^{-1}), which was obtained at a higher (75 *vs.* 50 mmol L^{-1}) sodium ion (Na^+) concentration.[15] Indeed, this provides a first indication of the substantial sensitivity to monovalent cations in the pressure dependences of both kinetic rates and equilibrium constants for DNA hybridization. By way of confirmation, we have determined the overall molar volume change upon hybridization under similar buffer conditions ([Na^+] = 75 mmol L^{-1}) to be ΔV^0 = +25.9(19) mL mol^{-1}, which is now in good agreement with previous published results. Detailed

 This journal is © the Owner Societies 2020

Published on 05 October 2020. Downloaded by University of Colorado at Boulder on 5/26/2021 9:49:42 PM.

studies on the dependence of these molar volumes on monovalent and divalent cation conditions are described below.

IIIC. Effects of Na^+ on pressure dependent folding kinetics

With one phosphate group per nucleotide, DNA is highly negatively charged under pH neutral conditions; therefore cations are essential to facilitate the formation of a more compact folded DNA configuration.[25,26] Moreover, charge screening and neutralization can have significant impacts on the hydration structure,[27] which in turn can alter the effective molar volume of the biomolecule plus solvent system and ultimately pressure dependences for the folding/unfolding kinetics.[28,29] In this section, pressure dependent equilibrium and kinetic rate constants of DNA hairpin folding are systematically investigated to explore the impact of monovalent Na^+ cations.

Firstly, the pressure dependence of the equilibrium constant K_{eq} as a function of $[Na^+]$ is displayed as a semi-logarithmic plot in Fig. 5. Under all conditions explored, the overall trend reveals linear decrease in $\ln(K_{eq})$ with elevated applied pressure, which by Eqn 3 predicts a positive $\Delta V^0 > 0$. However, there are two quite noticeable changes in $K_{eq}(P)$ with increasing $[Na^+]$: (i) $\ln(K_{eq})$ systematically shifts upward, reflecting that sodium significantly promotes folding of the DNA hairpin under all pressures; (ii) the $\ln(K_{eq})$ *vs.* P slopes become shallower with increasing $[Na^+]$, indicating an overall reduction in ΔV^0 and thus pressure sensitivity for DNA hairpin folding. From linear least squares fits, the resulting $[Na^+]$ dependent change in molar volume values are summarized in Table 1, which illustrate that ΔV^0 decreases systematically with increasing $[Na^+]$ up to 75 mmol L^{-1} values but eventually saturates at $[Na^+] \approx 75$ to 100 mmol L^{-1}. Note that ΔV^0 obtained at $[Na^+] = 75$ mmol L^{-1} is experimentally indistinguishable from the previous diffusion smFRET equilibrium measurements under the same salt conditions (25.9(19) *vs.* 23(2) mL mol^{-1}),[15] confirming that surface tethering has negligible impact on folding equilibrium properties for the DNA hairpin construct.[30,31]

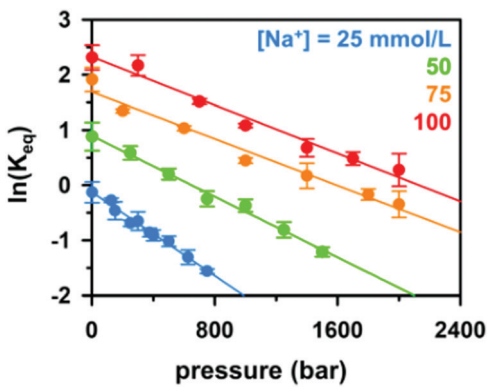

Fig. 5 Pressure dependent folding equilibrium constants (K_{eq}) as a function of Na^+ concentration, expressed as a van't Hoff pressure analysis, whereby the slope of these plots can be used to infer changes in the molar volume with uncertainties ($\approx$1 to 2 mL mol^{-1}) at $\approx$5 to 10% of a single H_2O molecule volume ($V \approx 18$ mL mol^{-1}).

Table 1 Na^+ dependence of overall molar volume changes (ΔV^0) for the single molecule DNA hairpin construct in the absence of divalent cation (*i.e.*, $[Mg^{2+}] = 0$)

$[Na^+]$ (mmol L^{-1})	25	50	75	100
ΔV^0 (mL mol^{-1})	46.4(19)	33.7(13)	25.9(19)	26.7(17)

Secondly, access to dwell time analysis in a surface tethered smFRET experiment also permits $[Na^+]$ dependent kinetic information to be obtained from the single-molecule E_{FRET} trajectories. The resulting pressure dependent rate constants k_{fold} and k_{unfold} from cumulative distribution functions are presented in Fig. 6A and B, respectively, as a function of $[Na^+]$. In these semi-logarithmic plots, the clear upward and downward vertical shifts in k_{fold} and k_{unfold} reveal that Na^+ promotes DNA hairpin folding by simultaneously increasing k_{fold} and decreasing k_{unfold}, respectively.[20] The plots for $\ln(k_{fold})$ *vs.* pressure in Fig. 6A are well fit to a series of nearly parallel lines with negative slopes, confirming that k_{fold} decreases with increasing pressure and $\Delta V^{\ddagger}_{fold} > 0$ for all $[Na^+]$ conditions explored (eqn (2)). The steepening of slopes for lowest $[Na^+]$ reflects a larger $\Delta V^{\ddagger}_{fold}$ at $[Na^+] < 75$ mmol L^{-1}, which then quickly decreases to a saturation value independent of increasing $[Na^+]$ (see also Table 2). Conversely, as evident from the positive slopes in Fig. 6B, $\ln(k_{unfold})$ increases rapidly with increasing pressure, consistent with a negative $\Delta V^{\ddagger}_{unfold} < 0$. Moreover, the sensitivity of k_{unfold} to pressure and cation

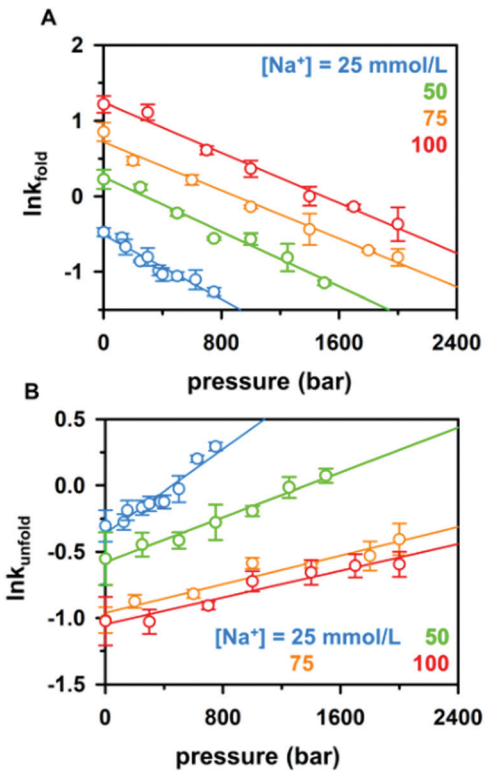

Fig. 6 Pressure dependent van't Hoff analysis of (A) folding (k_{fold}) and (B) unfolding (k_{unfold}) rate constants for a series of monovalent Na^+ concentrations.

Published on 05 October 2020. Downloaded by University of Colorado at Boulder on 5/26/2021 9:49:42 PM.

Table 2 Na^+ dependence of $\Delta V^{\ddagger}_{fold}$ and $\Delta V^{\ddagger}_{unfold}$ molar volume changes for the single molecule DNA hairpin construct in the absence of divalent cation (*i.e.*, $[Mg^{2+}] = 0$)

$[Na^+]$ (mmol L^{-1})	25	50	75	100
$\Delta V^{\ddagger}_{fold}$ (mL mol^{-1})	26(2)	22.1(16)	19.6(11)	20.4(10)
$\Delta V^{\ddagger}_{unfold}$ (mL mol^{-1})	−19(2)	−10.3(6)	−6.6(7)	−6.2(7)

concentration is now clearly evident in the steeper slopes at low $[Na^+] < 75$ mmol L^{-1}, revealing a much more significant Na^+ dependence of $\Delta V^{\ddagger}_{unfold}$ in the low sodium regime. Similar to $\Delta V^{\ddagger}_{fold}$, as $[Na^+]$ increases, the magnitude of $\Delta V^{\ddagger}_{unfold}$ decreases and gradually reaches a saturation value at $[Na^+] \approx 75$ mmol L^{-1}. By way of summary, increasing $[Na^+]$ lowers the sensitivity of both k_{fold} and k_{unfold} to pressure by reduction in the magnitude of $\Delta V^{\ddagger}_{fold}$ and $\Delta V^{\ddagger}_{unfold}$, respectively, with much stronger effects observed for the latter. However, as $[Na^+]$ increases above $\approx$75 mmol L^{-1}, monovalent cation effects on the pressure dependent rate constants appear to saturate for both $\Delta V^{\ddagger}_{fold}$ and $\Delta V^{\ddagger}_{unfold}$.

IV. Discussion

IVA. Effective volume of the DNA hairpin increases along the folding path

The surface tether smFRET experiments (Fig. 1) performed in the high pressure capillary sample cell allow us to probe the kinetics of DNA hairpin folding with pressure as a controlled external variable up to $\approx$5 kilobar.[7,15] The E_{FRET} time trajectories are calculated from the resulting time-dependent Cy3/Cy5 fluorescent signals (Fig. 2) and analyzed by conventional thresholding methods to obtain dwell time distributions of the folded and unfolded states (Fig. 3).[18,19,23] First of all, visual inspection of the E_{FRET} trajectories (Fig. 2) clearly reveals that with increasing pressure, the DNA hairpin spends more time in the unfolded (low E_{FRET}) conformation. Such DNA unfolding at elevated pressures is commonly referred to as pressure denaturation,[8,9] which had been routinely observed in multiple protein[4,5] and nucleic acid[7,32–34] systems in previous high pressure equilibrium measurements. Pressure denaturation indicates that the thermodynamic volume of the system is larger for the folded *vs.* unfolded conformations ($\Delta V^0 = V_{fold} - V_{unfold} > 0$) and therefore according to Le Chatelier's principle, folding is disfavored at high pressures (eqn (3)).[35] Though still a topic of intense discussion, such a volume increase due to folding is commonly ascribed to a corresponding change in hydration structure for the surrounding solvating water molecules.[4,35] In essence, the total system volume can decrease with DNA unfolding, since the volume occupied by water in this temperature range decreases with greater ordering of the solvent molecules.[28,29] This greater ordering and thus decreased volume can occur upon DNA unfolding by exposing greater surface area and thus orienting more water molecules, for example, by stronger Coulombic interactions with the phosphate anion backbone. An alternate mechanism proposed for $\Delta V > 0$ behavior would be the formation of water-excluding hydrophobic voids upon folding,[36] which would then effectively induce the folded DNA to displace a greater molar volume in solution.

In the kinetic analysis, Fig. 4A explicitly reveals the origin of this pressure-induced denaturation as a simultaneous decrease in k_{fold} and increase in k_{unfold}. Such kinetic response implies that the effective transition state volume must be smaller than the fully folded state, yet larger than the unfolded state ($V_{unfold} < V_{TS} < V_{fold}$). In Fig. 7, the volumes of each of the three conformations are displayed with V_{unfold} referenced to zero, clearly revealing that the volume of the DNA hairpin increases monotonically along the folding coordinate. Similar trends have also been observed in some protein systems with pressure-jump[37,38] and high pressure ZZ-exchange NMR[39] studies. Indeed, it is not surprising that the transition state adopts an intermediate volume between the folded and unfolded configurational extremes. However, these experimental activation molar volumes ($\Delta V^{\ddagger}_{fold}$ and $\Delta V^{\ddagger}_{unfold}$) also contain additional information on changes in water solvation structure due to the conformational transition,[29,35] and thus may offer insights into the influence of cations on DNA hydration as a function of the hybridization/folding coordinate,[27] as discussed in Sections IVB and IVC.

In previous pressure dependent UV melting experiments, many nucleic acid double helices are found to be stabilized by pressure,[11,12] which at first seems in contradiction with recent high pressure single molecule studies with hairpins of shorter duplex regions (<10 base-pairs).[13–15,21] However, a strong correlation between thermal stability and pressure response also has been previously observed in these UV melting experiments,[6] suggesting that pressure destabilizes the helices with low thermal stability (*e.g.* $T_m \leq 50$ °C). Since our single molecule experiments are necessarily performed under conditions where folded and unfolded states are both thermally populated, the hairpins are much less thermally stable, with T_m close to the room temperature.[13–15,21] As a result, the pressure induced destabilization effects ($\Delta V^0 > 0$) characterized at the

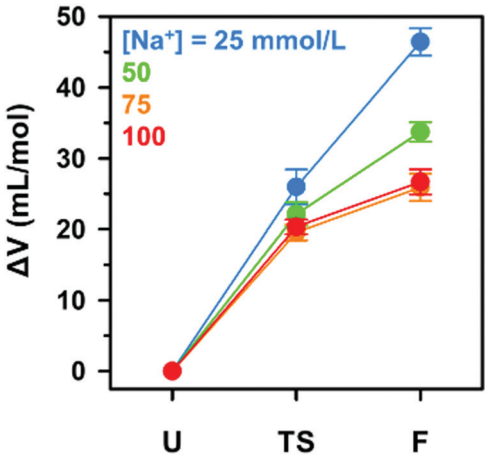

Fig. 7 Effective volume change along the folding coordinate as a function of increasing $[Na^+]$, with volume of the unfolded state (V_{unfold}) arbitrarily designated as the reference zero.

 This journal is © the Owner Societies 2020

Published on 05 October 2020. Downloaded by University of Colorado at Boulder on 5/26/2021 9:49:42 PM.

single molecule level are in fact quite consistent with previous observations in UV melting studies. Although the origins of the strong correlation between melting temperature and pressure response are not yet completely understood, it is thought to be accounted for by complex temperature and pressure dependent interactions involved in the helix-coil transition[6] such as hydration, base stacking, hydrogen bonding and Coulombic interactions, *etc.*[40] We note that the temperature-dependence of this pressure response has also been studied for nucleic acids in previous smFRET experiments.[34]

In addition to thermodynamic properties, the kinetics of helix-coil transition can be obtained by analysis of hysteresis in the UV melting/annealing curves.[41] The results again are consistent with $\Delta V^0 < 0$ for most of the duplex sequences studied,[42,43] while the signs of $\Delta V^{\ddagger}_{\text{fold/unfold}}$ may vary.[43] Moreover, the parameters in nearest neighbor expressions for ΔV^0 and $\Delta V^{\ddagger}_{\text{fold/unfold}}$ have been determined, with experiment and theory in good agreement for the duplex systems studied.[43] However, the same nearest neighbor analysis overpredicts ΔV^0 and $\Delta V^{\ddagger}_{\text{fold}}$ for the duplex sequence in our hairpin construct to be 0.0 mL mol^{-1} (*cf.*, +25.9 mL mol^{-1} at [Na^+] = 75 mM) and −1.5 mL mol^{-1} (*cf.*, +19.6 mL mol^{-1}). Although such discrepancies may be partially attributed to different buffer conditions and presence of the poly(dA) linker (which contributes ≈10 mL mol^{-1} to ΔV^0,[15]) such a nearest neighbor analysis is not expected to corroborate our results due simply to the fact that these parameters are derived from more thermally stable duplex structures that become stabilized under high pressure. Indeed, a more sophisticated high pressure smFRET experimental setup to study molecular DNA duplex formation[44] may be needed to rationalize the disparate pressure effects on short and long duplex sequences. Nevertheless, the current high pressure smFRET apparatus provides an extremely powerful tool to study the pressure dependent kinetics independent of thermal contributions, with the results obtained at near room temperatures better representing the impact of extreme pressures on deep sea organisms.

IVB. Na^+ decreases the activation volumes for both folding and unfolding pathways

The pressure responsive DNA folding equilibrium and kinetics have been studied at increasing [Na^+] to explore the monovalent cation effects (Fig. 6). The results are quantitatively summarized in Fig. 7, which reveals not only an strong increase in effective volume along the folding coordinate, but also that the presence of monovalent cation (Na^+) reduces these changes in volume and saturates above 75 mmol L^{-1}. Specifically, the most dramatic effects are observed in the volume change from the transition state to the folded state ($V_{\text{fold}} - V_{\text{TS}} = -\Delta V^{\ddagger}_{\text{unfold}}$), which collapses by 3-fold from +19(2) mL mol^{-1} to +6.2(7) mL mol^{-1} as [Na^+] increases from 25 to 100 mmol L^{-1}. It is worth noting that the exceptionally large dynamic range of pressures explored in these experiments results in ΔV uncertainties down at the ≈1 to 2 mL mol^{-1} level. For a sense of scale, this is roughly 5 to 10% the volume of a single H_2O molecule, which in turn allows us to explore and quantify the even smaller changes in molar volume induced by the presence of monovalent cations.

In particular, there is a quite significant Na^+ dependence to the change in thermodynamic molar volume (ΔV_s, Tables 1 and 2) which provides additional confirmation that hydration waters play a crucial role in pressure induced denaturation phenomena for DNA.[4,29,35] By way of a specific physical mechanism, monovalent cation association would tend to Debye shield the highly negatively charged DNA phosphate backbone,[45,46] weakening the coulombic interactions that align the water molecules and therefore allowing DNA to adopt a more weakly bound solvation shell with a larger effective volume.[28,29] Furthermore, such an increase in cation-induced volume changes could vary for each folding stage,[7] resulting in cation dependent changes in molar volume. In particular, since the more folded DNA hairpin has higher charge density and smaller water-exposed surface area,[47] the cations would be expected to more readily associate with and therefore saturate the ion atmospheres of the folded *vs.* unfolded structures at progressively lower concentrations.[48,49] Alternately stated, V_{unfold} increases faster than V_{fold} with increasing [Na^+] due to preferential cation association with the unfolded state,[50,51] resulting in an overall reduction in ΔV^0 ($\Delta\Delta V^0 < 0$). Moreover, similar monovalent cation effects can also be expected with respect to changes in the transition state volume (V_{TS}), which similarly predicts decreases in magnitudes of both $\Delta V^{\ddagger}_{\text{fold}}$ and $\Delta V^{\ddagger}_{\text{unfold}}$ with increasing [Na^+].

In previous thermodynamic and kinetic characterizations of DNA duplex formation,[44] increasing [Na^+] is found to simultaneously decrease the relative entropies for both the unfolded and transition state, indicating that Na^+ may promote more organized DNA structures in both conformations prior to folding.[44] In the present work, the volumetric measurements clearly reveal a significant decrease in the value of $V_{\text{fold}} - V_{\text{unfold}}$ as the predominant cation response (Fig. 7), or (for a smooth dependence on folding reaction coordinate) an increase in molar volume between the unfolded and folding transition state. In this context, our high pressure volumetric analysis of the [Na^+] dependence is consistent with a simple physical picture that Na^+ promotes the stability of a progressively more ''folded-like'' DNA structure by changes in hydration for both the unfolded, transition state, and folded configurations, an interpretation which is in good agreement with previous and current thermodynamic data.[44]

IVC. Cation-independent volume changes at physiological salt concentrations

The volumetric measurements for the DNA folding kinetics support that such monovalent cation effects saturate at ≈75 mmol L^{-1} for both $\Delta V^{\ddagger}_{\text{fold}}$ and $\Delta V^{\ddagger}_{\text{unfold}}$, which is comparable to physiological monovalent cation concentration conditions ([M^+] ≈ 100 mmol L^{-1}). The results therefore predict that significant [M^+] dependence in molar volume changes (ΔV_s) can only be observed under low salt conditions (*i.e.*, [M^+] < 100 mmol L^{-1}). Indeed, previous reports for the K^+-dependence of ΔV^0 in the DNA hairpin indicate folding only in the low monovalent cation regime ([M^+] < 30 mmol L^{-1}).[21] On the

Published on 05 October 2020. Downloaded by University of Colorado at Boulder on 5/26/2021 9:49:42 PM.

other hand, cesium ions (Cs^+) have been shown to reduce the volume changes at low concentration in previous high pressure poly[d(A-T)] melting experiments, with the effects saturating at $[Cs^+] \approx 100$ mmol L^{-1}.[11] However, we note in the same study that the ΔV^0 dependence on Na^+ does not show evidence of any saturation up to $[Na^+] = 1$ mol L^{-1}. We believe that sodium-promoted base stacking in the DNA poly(dA) single strand may be significantly perturbing the helix-coil transition and therefore resulting in additional salt-induced volume changes upon melting.[15,52] Clearly more high pressure data will be needed to fully explore and understand the potential salt/structure dependence of this saturation phenomenon.

Since magnesium (Mg^{2+}) is the most abundant divalent cation inside cells and known to significantly influence nucleic acid secondary and tertiary structure,[26,53] similar volumetric analyses have been performed as a function of $[Mg^{2+}] = 0$ to 0.75 mmol at background monovalent levels of $[Na^+] = 50$ mmol L^{-1} and $[K^+] = 25$ mmol L^{-1} (see ESI†), and the results are summarized in Fig. 8. The background monovalent cation mimics the physiological environment of DNA folding, provides additional stability for the folded DNA hairpin, which in turn increases the dynamic range of pressures accessible to the smFRET experiments. Interestingly, the molar volume folding landscape is only very slightly perturbed by the presence of Mg^{2+}, with $\Delta V^{\ddagger}_{fold}$ being completely independent and with only quite modest (<5 to 10%) changes in $\Delta V^{\ddagger}_{unfold}$ as a function of $[Mg^{2+}]$. We stress that this does not mean that divalent magnesium effects on the molar volume changes are necessarily weaker than monovalent sodium. Instead, it could be that the overall cation effects are effectively saturated at background monovalent levels of $[M^+] = 75$ mmol L^{-1} and that the additional magnesium is unable to achieve any further reduce in ΔV. We note that although the pressure dependent response (ΔV, from slopes) for hairpin folding is only weakly dependent on $[Mg^{2+}]$, the presence of magnesium still very strongly stabilizes the folded hairpin structure, as confirmed by large upward (and largely parallel) displacements in the $\log(K_{eq})$ *vs.* P plots exhibited in Fig. S1 (ESI†). To summarize, our data suggest under sufficiently high monovalent ($[M^+] \approx 100$ mmol L^{-1}) and divalent ($[M'^{2+}] \approx 1$ mmol L^{-1}) salt conditions, the molar volume changes (ΔV_s) for hybridization of the DNA hairpin saturate and depend only weakly on further increase in cation concentrations. By way of additional evidence, previous pressure dependent single molecule studies of the RNA lysine riboswitch reveal ΔV^0 also to be independent of salt under physiological conditions ($[Na^+] = 100$ to 500 mmol L^{-1}, $[Mg^{2+}] = 0.5$ to 1.5 mmol L^{-1}).[7] Although more data are clearly needed, the results thus far encourage expectations that cationic effects on RNA folding will exhibit a similar saturation behavior as seen in DNA.

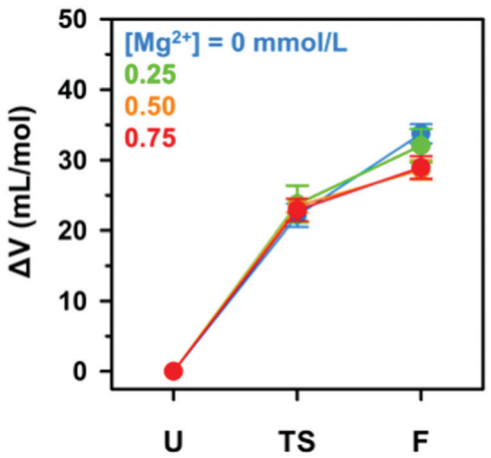

Fig. 8 Effective volume change along the folding coordinate as a function of increasing $[Mg^{2+}]$, with volume of the unfolded state (V_{unfold}) arbitrarily designated as the reference zero. Background $[Na^+] = 50$ mmol L^{-1}.

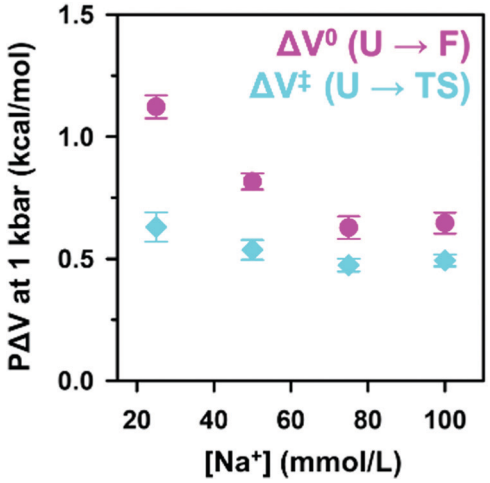

Fig. 9 $P\Delta V$ reversible work evaluated at $P = 1000$ bar to highlight the magnitude of free energy contributions ($kT \approx 0.6$ kcal mol^{-1}) induced by deep sea pressures as a function of increasing $[Na^+]$.

As a final comment in this subsection, we can translate these changes in molar volume (ΔV^0 and $\Delta V^{\ddagger}_{fold}$) into corresponding change in free energy landscapes. These reversible work contributions to free energy are specifically evaluated at a nominal $P = 1$ kilobar and plotted in Fig. 9 against $[Na^+]$ to highlight (i) effects of pressure-induced denaturation in deep sea (≈10 000 m) environments, and (ii) the saturation of the monovalent cation effects under physiological relevant conditions (Fig. 9). It is worth noting that even with ΔV^0 values only slightly larger than the size of a single water molecule ($V \approx 18$ mL mol^{-1}), the equivalent amount of reversible $P\Delta V$ work under such deep sea pressure conditions already contributes at the level of +1 kcal mol^{-1} (≈+2kT) to the overall folding free energy, thereby strongly shifting the equilibrium to the unfolded conformation. Furthermore, roughly half of that overall increase in free energy to folding is achieved by the transition state, which corresponds to a roughly three-fold deceleration in DNA hybridization rate constants under deep-sea environment *vs.* ambient pressure conditions.

IVD. Na^+ stabilization effects on DNA secondary structure revisited

In previous sections, we have mostly focused on the slopes in semi-logarithmic plots of K_{eq} or k *vs.* P (Fig. 5 and 6), whereby

 This journal is © the Owner Societies 2020

Published on 05 October 2020. Downloaded by University of Colorado at Boulder on 5/26/2021 9:49:42 PM.

changes in molar volume can be directly extracted from the pressure dependence. In addition to reducing ΔV_s, sodium also promotes DNA hairpin folding under all pressures explored by simultaneously increasing and decreasing k_{fold} and k_{unfold}, respectively, as shown in the vertical displacements in Fig. 5 and 6. For simplicity, we first focus on monovalent Na^+ effects at ambient pressure summarized in Fig. 10, whereby the folding (ΔG^0) and activation ($\Delta G^{\ddagger}$) free energies for this DNA hairpin are plotted against [Na^+]. In obtaining these values, we have used standard thermodynamic and transition state expressions relating overall ($\Delta G^0 = -kT\ln[K_{eq}]$) and transition state ($\Delta G^{\ddagger} = -kT\ln[k_{fold}/\nu]$) free energies to the equilibrium and rate constants measured. ν is an approximate attempt frequency for achieving the transition state, whose precise value is irrelevant in Fig. 10 for changes in free energies ($\Delta\Delta G^0$). The monotonic decrease in ΔG^0 with [Na^+] confirms that the folded DNA hairpin is energetically favored by increasing monovalent cation concentration. Furthermore, such a quasilinear decrease in ΔG^0 with [Na^+] is also consistent with empirical observations by Pegram *et al.* of cation effects on DNA folding in the low concentration regime ([M^+] $\approx$ 100 mmol L^{-1}),[47] with the slopes ($\partial\Delta G^0/\partial[M^+]$) strongly correlating with strength of solute–nucleic acid interactions and the change in solvent accessible surface area (ASA) during folding (ΔASA). Indeed, cations are known to accumulate on the surface of DNA through Coulombic attraction,[45,54,55] and in turn facilitate the formation of a more compact structure by charge neutralization and screening effects.[25,26] Moreover, similar sodium dependence is also observed in $\Delta G^{\ddagger}$ but with $\approx$50% shallower slopes, most simply attributed to fractionally smaller ΔASA‡ values or molar volume changes ($\Delta V^{\ddagger}_{fold}$) at the transition state.

As a parting comment, we note that the empirical relation between ΔG and [Na^+] may deviate from a simple linear function at low [Na^+] < 75 mmol as pressure-induced denaturation becomes more significant at higher pressures (Fig. 9). In other words, increased Na^+ could in principle protect the DNA structure from pressure-induced denaturation by both (i) increasing the hybridization stability and (ii) suppressing the pressure-induced dehybridization response. It is important to stress, however, that such effects would not necessarily make sodium (or other cations) suitable candidates to help deep sea organisms maintain cellular function at extreme pressures, due to the fact that high cation concentrations can interact strongly with biomolecules in cells and thus highly perturb their function,[56] as in dynamic gene regulation by RNA riboswitches.[7] Instead of recruiting cations, therefore, deep sea organisms accumulate high concentrations of small organic solutes (*e.g.* trimethylamine *N*-oxide, TMAO) that are much more compatible with biomolecule structure/function[10] and can thereby counteract these pressure-induced free energy contributions primarily by reducing the pressure sensitivity to biomolecule conformation.[7,21,57,58]

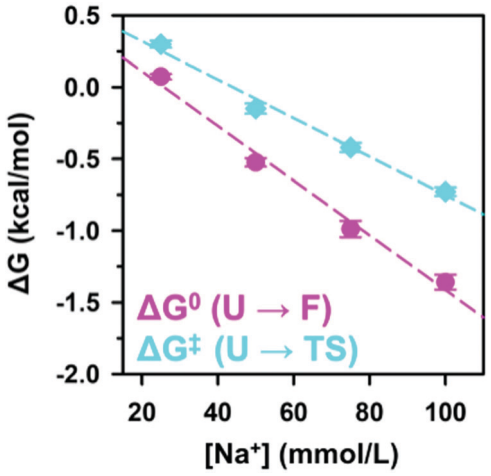

Fig. 10 Na^+ stabilization effects on the DNA hairpin secondary structure under ambient pressure conditions.

V. Summary and conclusion

First high pressure kinetic studies of DNA hybridization at the single molecule level have been investigated by smFRET experiments on a doubly dye labelled DNA hairpin construct over a wide dynamic range of external pressures (1 to 1500 bar). The resulting E_{FRET} time trajectories from the prolonged observation of single tethered molecule fluorescence allows us to extract information on the unimolecular rate of DNA hairpin folding/unfolding. The folding (k_{fold}) and unfolding (k_{unfold}) rate constants are found to simultaneously decrease and increase, respectively with increasing pressure, resulting in predictions consistent with pressure-induced denaturation of DNA secondary structure and in excellent agreement with previous equilibrium high pressure studies on freely diffusing constructs. By way of pressure dependent van't Hoff analysis, the effective volume of the DNA plus solvent system is found to systematically increase along the folding coordinate ($V_{unfold} < V_{TS} < V_{fold}$), with volume sensitivities and experimental uncertainties (1 to 2 mL mol^{-1}) on the order of 5 to 10% of a single H_2O molecule. Since the cation may significantly change the hydration structure and consequently the effective volume of the DNA plus solvent system, the change in free activation volumes for both folding and unfolding ($\Delta V^{\ddagger}_{fold}$ and $\Delta V^{\ddagger}_{unfold}$) are shown to decrease at low [Na^+] and gradually reach saturation limits at [Na^+] $\approx$ 75 mmol L^{-1}. The more significant reduction in $\Delta V^{\ddagger}_{unfold}$ indicates a greater resemblance between V_{TS} and V_{fold}, which in turn signifies that Na^+ is able to facilitate a more folded-like transition state configuration prior to formation of the fully folded DNA hairpin. Finally, both $\Delta V^{\ddagger}_{fold}$ and $\Delta V^{\ddagger}_{unfold}$ are approximately insensitive to monovalent (Na^+) and divalent (Mg^{2+}) cations under near-physiological salt concentrations, suggesting cation effects on these changes on molar volume (ΔV_s) may saturate *in vivo* and therefore be insensitive to moderate intracellular cation fluctuation.

Conflicts of interest

There are no conflicts to declare.

Published on 05 October 2020. Downloaded by University of Colorado at Boulder on 5/26/2021 9:49:42 PM.

Acknowledgements

Primary funding for this work has been provided by the National Science Foundation: Chemical, Structure, Dynamics and Mechanisms-A Program (CHE-1665271), with support eventually transitioning to the Air Force Office of Scientific Research (FA9550-15-1-0090). We would also like to acknowledge early contributions to apparatus development by National Science Foundation Physics Frontier Center (PHY 1734006) and the W. M. Keck Foundation Initiative in RNA Sciences at the University of Colorado, Boulder.

References

1 A. A. Yayanos, A. S. Dietz and R. Van Boxtel, Obligately Barophilic Bacterium from the Mariana Trench, *Proc. Natl. Acad. Sci. U. S. A.*, 1981, **78**(8), 5212–5215.
2 C. Kato, L. Li, Y. Nogi, Y. Nakamura, J. Tamaoka and K. Horikoshi, Extremely Barophilic Bacteria Isolated from the Mariana Trench, Challenger Deep, at a Depth of 11,000 Meters, *Appl. Environ. Microbiol.*, 1998, **64**(4), 1510–1513.
3 G. N. Somero, Adaptations to High Hydrostatic Pressure, *Annu. Rev. Physiol.*, 1992, **54**(1), 557–577.
4 M. Gross and R. Jaenicke, Proteins Under Pressure, *Eur. J. Biochem.*, 1994, **221**(2), 617–630.
5 V. V. Mozhaev, K. Heremans, J. Frank, P. Masson and C. Balny, High Pressure Effects on Protein Structure and Function, *Proteins*, 1996, **24**(1), 81–91.
6 D. N. Dubins, A. Lee, R. B. Macgregor and T. V. Chalikian, On the Stability of Double Stranded Nucleic Acids, *J. Am. Chem. Soc.*, 2001, **123**(38), 9254–9259.
7 H.-L. Sung and D. J. Nesbitt, High Pressure Single-Molecule FRET Studies of the Lysine Riboswitch: Cationic and Osmolytic Effects on Pressure Induced Denaturation, *Phys. Chem. Chem. Phys.*, 2020, **22**(28), 15853–15866.
8 A. Zipp and W. Kauzmann, Pressure denaturation of metmyoglobin, *Biochemistry*, 1973, **12**(21), 4217–4228.
9 J. Roche and C. A. Royer, Lessons from Pressure Denaturation of Proteins, *J. R. Soc., Interface*, 2018, **15**(147), 20180244.
10 P. H. Yancey, W. R. Blake and J. Conley, Unusual Organic Osmolytes in Deep-Sea Animals: Adaptations to Hydrostatic Pressure and Other Perturbants, *Comp. Biochem. Physiol., Part A: Mol. Integr. Physiol.*, 2002, **133**(3), 667–676.
11 R. Najaf-Zadeh, J. Q. Wu and R. B. Macgregor, Effect of Cations on the Volume of the Helix-Coil Transition of poly[d(A-T)], *Biochim. Biophys. Acta, Gene Struct. Expression*, 1995, **1262**(1), 52–58.
12 J. Q. Wu and R. B. Macgregor Jr, Pressure Dependence of the Helix–Coil Transition Temperature of poly[d(G-C)], *Biopolymers*, 1995, **35**(4), 369–376.
13 S. Patra, C. Anders, N. Erwin and R. Winter, Osmolyte Effects on the Conformational Dynamics of a DNA Hairpin at Ambient and Extreme Environmental Conditions, *Angew. Chem.*, 2017, **56**(18), 5045–5049.
14 S. Patra, C. Anders, P. H. Schummel and R. Winter, Antagonistic Effects of Natural Osmolyte Mixtures and Hydrostatic Pressure on the Conformational Dynamics of a DNA Hairpin Probed at the Single-Molecule Level, *Phys. Chem. Chem. Phys.*, 2018, **20**(19), 13159–13170.
15 H.-L. Sung and D. J. Nesbitt, DNA Hairpin Hybridization under Extreme Pressures: A Single-Molecule FRET Study, *J. Phys. Chem. B*, 2020, **124**(1), 110–120.
16 T. Pan and T. Sosnick, RNA Folding During Transcription, *Annu. Rev. Biophys. Biomol. Struct.*, 2006, **35**(1), 161–175.
17 M. L. Mott and J. M. Berger, DNA Replication Initiation: Mechanisms and Regulation in Bacteria, *Nat. Rev. Microbiol.*, 2007, **5**(5), 343–354.
18 J. H. Hodak, J. L. Fiore, D. J. Nesbitt, C. D. Downey and A. Pardi, Docking Kinetics and Equilibrium of a GAAA Tetraloop-Receptor Motif Probed by Single-Molecule FRET, *Proc. Natl. Acad. Sci. U. S. A.*, 2005, **102**(30), 10505–10510.
19 A. Sengupta, H.-L. Sung and D. J. Nesbitt, Amino Acid Specific Effects on RNA Tertiary Interactions: Single-Molecule Kinetic and Thermodynamic Studies, *J. Phys. Chem. B*, 2016, **120**(41), 10615–10627.
20 D. A. Nicholson, A. Sengupta, H.-L. Sung and D. J. Nesbitt, Amino Acid Stabilization of Nucleic Acid Secondary Structure: Kinetic Insights from Single-Molecule Studies, *J. Phys. Chem. B*, 2018, **122**(43), 9869–9876.
21 S. Patra, V. Schuabb, I. Kiesel, J.-M. Knop, R. Oliva and R. Winter, Exploring the Effects of Cosolutes and Crowding on the Volumetric and Kinetic Profile of the Conformational Dynamics of a poly dA loop DNA Hairpin: A Single-Molecule FRET Study, *Nucleic Acids Res.*, 2018, **47**(2), 981–996.
22 R. Tsukanov, T. E. Tomov, R. Masoud, H. Drory, N. Plavner, M. Liber and E. Nir, Detailed Study of DNA Hairpin Dynamics Using Single-Molecule Fluorescence Assisted by DNA Origami, *J. Phys. Chem. B*, 2013, **117**(40), 11932–11942.
23 H.-L. Sung and D. J. Nesbitt, Single-Molecule FRET Kinetics of the Mn2+ Riboswitch: Evidence for Allosteric Mg2+ Control of ''Induced-Fit'' vs ''Conformational Selection'' Folding Pathways, *J. Phys. Chem. B*, 2019, **123**(9), 2005–2015.
24 H.-X. Zhou, Rate Theories for Biologists, *Q. Rev. Biophys.*, 2010, **43**(2), 219–293.
25 M. T. Record Jr, Effects of Na^+ and Mg^{++} Ions on the Helix–Coil Transition of DNA, *Biopolymers*, 1975, **14**(10), 2137–2158.
26 R. Owczarzy, B. G. Moreira, Y. You, M. A. Behlke and J. A. Walder, Predicting Stability of DNA Duplexes in Solutions Containing Magnesium and Monovalent Cations, *Biochemistry*, 2008, **47**(19), 5336–5353.
27 V. Buckin, H. Tran, V. Morozov and L. A. Marky, Hydration Effects Accompanying the Substitution of Counterions in the Ionic Atmosphere of Poly(rA)·Poly(rU) and Poly(rA)·2Poly(rU) Helices, *J. Am. Chem. Soc.*, 1996, **118**(30), 7033–7039.
28 R. d. C. Barbosa and M. C. Barbosa, Hydration Shell of the TS-Kappa Protein: Higher Density than Bulk Water, *Physica A*, 2015, **439**, 48–58.
29 T. V. Chalikian, A. P. Sarvazyan, G. E. Plum and K. J. Breslauer, Influence of Base Composition, Base Sequence, and Duplex Structure on DNA Hydration: Apparent Molar Volumes and Apparent Molar Adiabatic Compressibilities of Synthetic and

 This journal is © the Owner Societies 2020

Published on 05 October 2020. Downloaded by University of Colorado at Boulder on 5/26/2021 9:49:42 PM.

Natural DNA Duplexes at 25 °C, *Biochemistry*, 1994, **33**(9), 2394–2401.

30 J. L. Fiore, B. Kraemer, F. Koberling, R. Edmann and D. J. Nesbitt, Enthalpy-Driven RNA Folding: Single-Molecule Thermodynamics of Tetraloop−Receptor Tertiary Interaction, *Biochemistry*, 2009, **48**(11), 2550–2558.

31 E. D. Holmstrom, J. T. Polaski, R. T. Batey and D. J. Nesbitt, Single-Molecule Conformational Dynamics of a Biologically Functional Hydroxocobalamin Riboswitch, *J. Am. Chem. Soc.*, 2014, **136**(48), 16832–16843.

32 C. D. Downey, R. L. Crisman, T. W. Randolph and A. Pardi, Influence of Hydrostatic Pressure and Cosolutes on RNA Tertiary Structure, *J. Am. Chem. Soc.*, 2007, **129**(30), 9290–9291.

33 S. Takahashi and N. Sugimoto, Effect of Pressure on Thermal Stability of G-Quadruplex DNA and Double-Stranded DNA Structures, *Molecules*, 2013, **18**(11), 13297–13319.

34 L. Arns, J.-M. Knop, S. Patra, C. Anders and R. Winter, Single-Molecule Insights into the Temperature and Pressure Dependent Conformational Dynamics of Nucleic Acids in the Presence of Crowders and Osmolytes, *Biophys. Chem.*, 2019, **251**, 106190.

35 T. V. Chalikian and K. J. Breslauer, On Volume Changes Accompanying Conformational Transitions of Biopolymers, *Biopolymers*, 1996, **39**(5), 619–626.

36 J. Roche, J. A. Caro, D. R. Norberto, P. Barthe, C. Roumestand, J. L. Schlessman, A. E. Garcia, E. García-Moreno, B. Royer and C. A. Cavities, Determine the Pressure Unfolding of Proteins, *Proc. Natl. Acad. Sci. U. S. A.*, 2012, **109**(18), 6945–6950.

37 C.-Y. Tan, C.-H. Xu, J. Wong, J.-R. Shen, S. Sakuma, Y. Yamamoto, R. Lange, C. Balny and K.-C. Ruan, Pressure Equilibrium and Jump Study on Unfolding of 23-kDa Protein from Spinach Photosystem II, *Biophys. J.*, 2005, **88**(2), 1264–1275.

38 J. Font, J. Torrent, M. Ribó, D. V. Laurents, C. Balny, M. Vilanova and R. Lange, Pressure-Jump-Induced Kinetics Reveals a Hydration Dependent Folding/Unfolding Mechanism of Ribonuclease A, *Biophys. J.*, 2006, **91**(6), 2264–2274.

39 Y. Zhang, S. Kitazawa, I. Peran, N. Stenzoski, S. A. McCallum, D. P. Raleigh and C. A. Royer, High Pressure ZZ-Exchange NMR Reveals Key Features of Protein Folding Transition States, *J. Am. Chem. Soc.*, 2016, **138**(46), 15260–15266.

40 Y.-K. Cheng and B. M. Pettitt, Stabilities of Double- and Triple-strand Helical Nucleic Acids, *Prog. Biophys. Mol. Biol.*, 1992, **58**(3), 225–257.

41 M. Rougee, B. Faucon, J. L. Mergny, F. Barcelo, C. Giovannangeli, T. Garestier and C. Helene, Kinetics and Thermodynamics of Triple-Helix Formation: Effects of Ionic Strength and Mismatched, *Biochemistry*, 1992, **31**(38), 9269–9278.

42 M.-C. Lin and R. B. Macgregor, Activation Volume of DNA Duplex Formation, *Biochemistry*, 1997, **36**(21), 6539–6544.

43 D. N. Dubins and R. B. Macgregor Jr., Volumetric Properties of the Formation of Double Stranded DNA: A Nearest-Neighbor Analysis, *Biopolymers*, 2004, **73**(2), 242–257.

44 N. F. Dupuis, E. D. Holmstrom and D. J. Nesbitt, Single-Molecule Kinetics Reveal Cation-Promoted DNA Duplex Formation Through Ordering of Single-Stranded Helices, *Biophys. J.*, 2013, **105**(3), 756–766.

45 R. Das, T. T. Mills, L. W. Kwok, G. S. Maskel, I. S. Millett, S. Doniach, K. D. Finkelstein, D. Herschlag and L. Pollack, Counterion Distribution around DNA Probed by Solution X-Ray Scattering, *Phys. Rev. Lett.*, 2003, **90**(18), 188103.

46 J. M. Tokuda, S. A. Pabit and L. Pollack, Protein-DNA and ion-DNA Interactions Revealed Through Contrast Variation SAXS, *Biophys. Rev.*, 2016, **8**(2), 139–149.

47 L. M. Pegram, T. Wendorff, R. Erdmann, I. Shkel, D. Bellissimo, D. J. Felitsky and M. T. Record, Why Hofmeister Effects of Many Salts Favor Protein Folding but not DNA Helix Formation, *Proc. Natl. Acad. Sci. U. S. A.*, 2010, **107**(17), 7716–7721.

48 W. H. Braunlin and V. A. Bloomfield, Proton NMR Study of the Base-Pairing Reactions of d(GGAATTCC): Salt Effects on the Equilibria and Kinetics of Strand Association, *Biochemistry*, 1991, **30**(3), 754–758.

49 C. H. Spink and J. B. Chaires, Effects of Hydration, Ion Release, and Excluded Volume on the Melting of Triplex and Duplex DNA, *Biochemistry*, 1999, **38**(1), 496–508.

50 R. Shiman and D. E. Draper, Stabilization of RNA Tertiary Structure by Monovalent Cations, *J. Mol. Biol.*, 2000, **302**(1), 79–91.

51 D. Leipply; D. Lambert and D. E. Draper, Chapter 21 - Ion–RNA Interactions: Thermodynamic Analysis of the Effects of Mono- and Divalent Ions on RNA Conformational Equilibria, *Methods in Enzymology*, Academic Press, 2009, vol. 469, pp. 433–463.

52 N. L. Goddard, G. Bonnet, O. Krichevsky and A. Libchaber, Sequence Dependent Rigidity of Single Stranded DNA, *Phys. Rev. Lett.*, 2000, **85**(11), 2400–2403.

53 A. Sreedhara and J. A. Cowan, Structural and Catalytic Roles for Divalent Magnesium in Nucleic Acid Biochemistry, *BioMetals*, 2002, **15**(3), 211–223.

54 M. Gebala, S. Bonilla, N. Bisaria and D. Herschlag, Does Cation Size Affect Occupancy and Electrostatic Screening of the Nucleic Acid Ion Atmosphere?, *J. Am. Chem. Soc.*, 2016, **138**(34), 10925–10934.

55 L. McFail-Isom, C. C. Sines and L. D. Williams, DNA Structure: Cations in Charge?, *Curr. Opin. Struct. Biol.*, 1999, **9**(3), 298–304.

56 P. H. Yancey, Organic Osmolytes as Compatible, Metabolic and Counteracting Cytoprotectants in High Osmolarity and Other Stresses, *J. Exp. Biol.*, 2005, **208**(15), 2819–2830.

57 P. H. Yancey, A. L. Fyfe-Johnson, R. H. Kelly, V. P. Walker and M. T. Auñón, Trimethylamine Oxide Counteracts Effects of Hydrostatic Pressure on Proteins of Deep-Sea Teleosts, *J. Exp. Zool.*, 2001, **289**(3), 172–176.

58 C. Krywka, C. Sternemann, M. Paulus, M. Tolan, C. Royer and R. Winter, Effect of Osmolytes on Pressure-Induced Unfolding of Proteins: A High-Pressure SAXS Study, *ChemPhysChem*, 2008, **9**(18), 2809–2815.